Recent progress on biodegradable materials and transient electronics

Rongfeng Li [1], Liu Wang [1], Deying Kong, Lan Yin*

School of Materials Science and Engineering, Tsinghua University, Beijing 100084 China

ARTICLE INFO

ABSTRACT

Transient electronics (or biodegradable electronics) is an emerging technology whose key characteristic is an ability to dissolve, resorb, or physically disappear in physiological environments in a controlled manner. Potential applications include eco-friendly sensors, temporary biomedical implants, and data-secure hardware. Biodegradable electronics built with water-soluble, biocompatible active and passive materials can provide multifunctional operations for diagnostic and therapeutic purposes, such as monitoring intracranial pressure, identifying neural networks, assisting wound healing process, etc. This review summarizes the up-to-date materials strategies, manufacturing schemes, and device layouts for biodegradable electronics, and the outlook is discussed at the end. It is expected that the translation of these materials and technologies into clinical settings could potentially provide vital tools that are beneficial for human healthcare.

1. Introductions

Electronics has made tremendous impacts on human society and has been widely used in almost every field, including tele-communication, entertainment, and healthcare, to name a few. While the long-lasting stable operation is a hallmark of conventional electronics, an emerging type of device that possesses "transient" function is gaining increasing attention recently [1–7]. Such devices are made of biodegradable materials, and can completely or partially dissolve, resorb or physically disappear after functioning in environmental or physiological conditions at controlled rates, and are termed as "transient electronics", or "biodegradable electronics" for biomedical or eco-friendly applications. Biodegradable electronics as temporary implants can be safely absorbed by the body after fulfilling its therapeutic and diagnostic functions, similar as biodegradable sutures or cardiovascular stents, and as a result eliminates second surgeries for device retrieval and decreases associated risks of infection. For green electronics, introducing biodegradability to consumer electronics or environmental monitors is expected to greatly alleviate landfill and environmental issues caused by electronic waste (E-waste,

more than 50 million tons each year) [8,9] and eliminate associated costs and risks resulting from recycling operations. Furthermore, transient devices capable of self-destruction that protect information from unauthorized access can be used as data-secure hardware.

Demonstrated transient devices so far are mostly associated with degradation in aqueous solutions targeting biomedical or environmental applications [1–4,10]. Researchers have performed studies on biodegradable materials for transient electronics, including materials dissolution chemistry, degradation modeling, fabrication techniques, device integration, etc. Early attempts have been focusing on organic materials including natural or synthesized biodegradable polymers, and partially degradable devices have been achieved with contributions mainly from substrate components [11–13]. Recent studies have showed that mono-crystalline silicon nanomembranes (mono-Si NMs) dissolve in physiological environments with rates ranging from a few nanometers to more than 100 nm per day [1,2,14,15], depending on the types of aqueous solutions. Together with degradable inorganic dielectrics, metals, and polymer substrates, dissolvable Si NMs enable fully biodegradable electronics with superior operation characteristics that can also be compatible with semiconductor foundry process [16,17]. Novel fabrication techniques have been developed to adapt the sensitive nature of biodegradable materials to device integration, preventing materials destruction by solvent, temperature, or water. A variety of fully biodegradable devices in physiological solutions have been demonstrated, including thermal

* Corresponding author.
E-mail address: lanyin@tsinghua.edu.cn (L. Yin).
Peer review under responsibility of KeAi Communications Co., Ltd.
[1] Equal contribution.

therapy device [1], intracranial pressure sensor (ICP) [18], electro-corticography (ECoG) recording systems [19], radio frequency (RF) electronics [20], batteries [21], drug delivery systems [22], etc. In order to achieve both stable operations for a certain period of time and then transience at a later stage, encapsulation materials are critically important. The functional lifetime of achieved transient devices is mostly defined by the degradation time and water permeability of encapsulation materials, and the thickness of active electronic components. External trigger stimulus (moisture, temperature, light, mechanical force, etc) represents an alternative factor to determine the starting point of transience, and demonstrated triggered degradation in non-aqueous environments are mostly associated with non-biological applications. In these scenarios, devices are either capable of full transience, or partial degradation.

As an emerging technology, transient electronics has made fast development since it has been first proposed on 2012 [1], and more possibilities are to be explored to further expand its opportunities to be used for healthcare and green electronics. This review summarizes recent progress on biodegradable materials and electronics, focusing on biomedical and eco-friendly applications. It is noted that most biodegradable electronics designed for biomedical applications can be well adapted for eco-friendly usage. A wide range of biodegradable materials will be first reviewed, followed by an introduction of various novel fabrication techniques. Representative biodegradable functional electronic systems and eco-friendly devices will be described, and perspectives to further advance high-performance multifunctional transient electronics will be discussed.

2. Materials

Biodegradable electronic materials capable of complete degradation and physical transience in physiological or environmental solutions have been studied in order to establish a comprehensive material database for the construction of biodegradable electronics. Biodegradable organic materials (natural or synthesized polymers) that have been extensively studied as biomedical implants (e.g. sutures, stents, scaffolds for regenerative medicine) often serve as passive components where the function is defined by their mechanics and structure. While inorganic semiconductors, metals, dielectrics are shown to have excellent degradation behavior as well as superior electronic properties. Combination of these two categories of materials enables high-performance active devices and sensors that can significantly expand the possible applications of biodegradable electronics. It is noted that although the degradation of inorganic materials has been studied for years in the context of corrosion science, most studies focus on materials in the bulk format and in relatively more corrosive environments (e.g. strong acid or basic solutions). Exploration of materials degradation in biological solutions in the thin film format relevant to electronics standards is therefore necessary, as well as establishing the correlations between materials degradation and electronic properties. Available studies have investigated the degradation rates of dissolvable thin film electronic materials, including semiconductors, dielectrics, metals, etc, mostly in de-ionized (DI) water and simulated bio-fluids such as phosphate buffered saline and phosphate buffered solutions. It is noted that the *in vitro* degradation behavior could be very different from the *in vivo* degradation due to the presence of complex components (e.g. proteins, cells). The influence of various *in vivo* components on the degradation behavior is under investigation, e.g. recent studies have shown that proteins can possibly slow down the dissolution rates of Si [23]. Biocompatibility of these materials has also been evaluated both *in vitro* and *in vivo* through cell toxicity tests and animal models.

Overall, the research on biodegradable materials for electronics is still in progress. Although materials candidates capable of full degradation have been proposed and various functional devices have been demonstrated, further materials studies are necessary, including extensive investigations of material interactions with components in real biological solutions (e.g. proteins, cells, etc), local enrichment of dissolution by-products and the associated biocompatibility, exploration of effective encapsulation materials, etc. In the following sections, materials proposed for biodegradable electronics are discussed in terms of semiconductors, dielectrics, metals, and substrate and encapsulation materials. Available modeling tools capturing materials degradation rates will also be given.

2.1. Semiconductors

Semiconducting materials are the most important component in electronics that determines the performance. Literature studies have showned that mono-Si NMs (30—300 nm), polycrystalline silicon (poly-Si), amorphous silicon (a-Si), germanium (Ge), silicon germanium alloy (SiGe), indium-gallium-zinc oxide (a-IGZO), and zinc oxide (ZnO) are dissolvable in physiological aqueous solutions [1,2,14,15,24,25]. Great efforts have been devoted to the investigation of dissolution mechanism of single crystal Si NMs in various bio-fluids and aqueous solutions, as Si offers excellent operational characteristics as well as alignment with the deep base of scientific and engineering knowledge associated with the well-established electronics industry. In order to investigate the dissolution kinetics of mono-Si NMs, arrays of Si NMs are fabricated on silicon oxide/silicon (SiO_2/Si) substrates using a commercially available silicon on insulator (SOI) wafer. The changes of the thickness of Si NMs are monitored as a function of time by profilometer or atomic force microscopy (AFM). Representative dissolution process of Si NMs in bovine serum is captured by the AFM as shown in Fig. 1(a) [14]. It is found that doping levels, pH, temperatures, concentrations and types of ions, and proteins in the solution can all have significant effects on the dissolution rates of mono-Si NMs, as shown in Fig. 1(b) and 1(d) [2,14,15,23]. Higher temperatures and pH levels speed up dissolution rates of Si NMs, while high doping levels ($>10^{20}$ cm^{-3}) significantly decrease the rates [2,14]. Moreover, chlorides and phosphates concentrations above a certain level greatly accelerate silicon dissolution even in a near-neutral aqueous solution (pH~7.5) [15]. A recent report suggests that the calcium concentration can significantly increases the dissolution rates, while the presence of silicic acid and proteins (albumin) slows down the reactions [23]. Density functional theory (DFT) and molecular dynamics (MD) simulation tools can be applied to reveal the underlying physics of silicon dissolution behavior [15]. It is found that silicon dissolution proceeds through the nucleophilic attack of silicon surface bonds, which weakens the interior bonds of surface silicon atoms (backbonds) and therefore increases their susceptibility to further ion attack, as shown in Fig. 1(c). Similarly, dissolution rates of poly-Si, a-Si, Ge, and SiGe are greatly affected by pH, temperatures, proteins and types of ions. For example, the rates of these materials at the physiological temperature (37 °C) are higher than those at room temperature. At similar pH, bovine serum leads to dissolution rates that are 30—40 times higher than those of a phosphate buffered solution at 37 °C for poly-Si, a-Si, and single crystal Si [24]. *In vitro* cytotoxicity studies on mono-Si, poly-Si, a-Si, Ge and SiGe materials, and *in vivo* studies of mono-Si membranes implanted in subdermal regions of BALB/c mice suggest good biocompatibility [2,14,24]. Besides the aforementioned inorganic semiconductors, PDPP-PD synthesized from diketopyrrolopyrrole (DPP) has recently been proposed as an eco-friendly, biocompatible
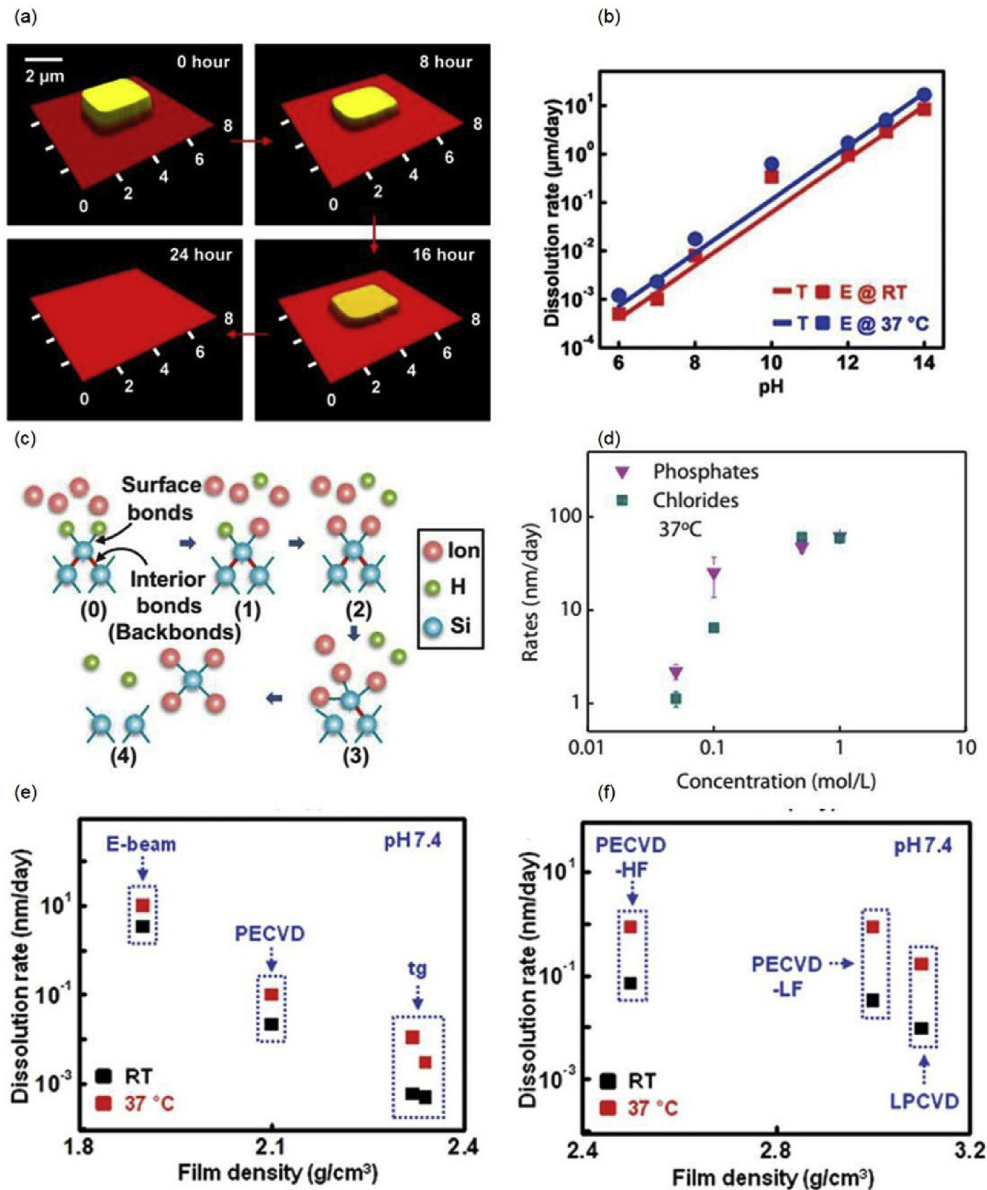
Fig. 1. (a) Images of dissolution of Si NMs at various stages in bovine serum (pH ~7.4, 37 °C) measured by AFM; (b) Dissolution rates of Si NMs at room temperature and 37 °C as a function of pH in buffer solutions, with E as the experimental results (E, symbols) and T as the modeling results (T, lines); (c) Schematic illustration of the dissolution mechanism of mono-Si: nucleophilic ions bonded to Si surface atoms weaken the interior bonds and assist Si dissolution; (d) Dissolution rates of Si NMs as a function of concentrations of phosphates and chlorides (pH ~7.5, 37 °C); (e) Dissolution rates of SiO_2 as a function of film density in buffer solutions at both room temperature and 37 °C; (f) Dissolution rates of Si_3N_4 as a function of film density in buffer solutions at both room temperature and 37 °C. Reprinted with permissions from Refs. [2, 14, 15, 27].

and totally disintegrable semiconducting material for transient electronics [26].

2.2. Dielectrics

Dielectric materials, including magnesium oxide (MgO), silicon dioxide (SiO_2), silicon nitride (Si_3N_4), and spin-on-glass (SOG) are all found to be biodegradable in aqueous solutions [1,27,28]. The kinetics of hydrolysis of these materials depends not only on pH levels, ion concentrations, and temperatures, but also on the density of the films which is determined by the deposition conditions. For instance, dissolution rates of oxides deposited by electron-beam (e-beam) evaporation are 100 times slower compared to those deposited by plasma-enhanced chemical vapor deposition (PECVD) method, as shown in Fig. 1(e) [27]. In terms of nitride, the

dissolution rates of low pressure chemical vapor deposition (LPCVD) nitride is slower than those of PECVD nitride, as shown in Fig. 1(f) [27].

2.3. Metals

Metals serving as electrode contacts and interlayer connections for electronics possess the advantage of high conductivity. Dissolution measurements of metallic nanomembranes (40–300 nm) have been investigated by monitoring the resistance changes as a function of time on patterned serpentine metal traces in solutions with different pH and at different temperatures, with the dissolution rates defined as electrical dissolution rates (EDRs) [29]. It is found that metallic thin films, including magnesium (Mg), zinc (Zn), molybdenum (Mo), and tungsten (W) can all dissolve in DI

water and simulated body fluids (Hanks' solution pH 5–8) with different rates. Dissolution rates of Mg and Zn thin films are much faster compared to those of Mo and W, and deposition conditions can have a great influence [29]. Fig. 2(a) shows the representative dissolution behavior of Mo in various pH and temperatures. Mo demonstrates slower dissolution rates with higher pH in Hanks' solutions. Surface chemistry and microstructure of Mo after dissolution in DI water for 40 hours appear in Fig. 2(b), and porous oxides are observed. In general, oxide formation is found on the surface of metals as dissolution proceeds, and the dissolution of metals is much faster compared to that of the residual oxides, e.g.

such oxides on Mg, AZ31B Mg alloy, and Zn of 300 nm fully disappear within a few days in DI water, while residue oxides on W (150 nm) and Mo (40 nm) can remain on substrates for weeks. Moreover, the dissolution of metallic thin films proceeds in a non-uniform manner, e.g. pitting corrosion or formation of micropores (Fig. 2(b)), and therefore metals lose their conductivity ahead of complete dissolution of materials. *In vivo* studies of Mg thin films in sub-dermal regions of BALB/c mice reveal good biocompatibility [2]. As will be shown later, implantation of devices using Mo components on a rat model indicates no significant immune reactions [18,19].
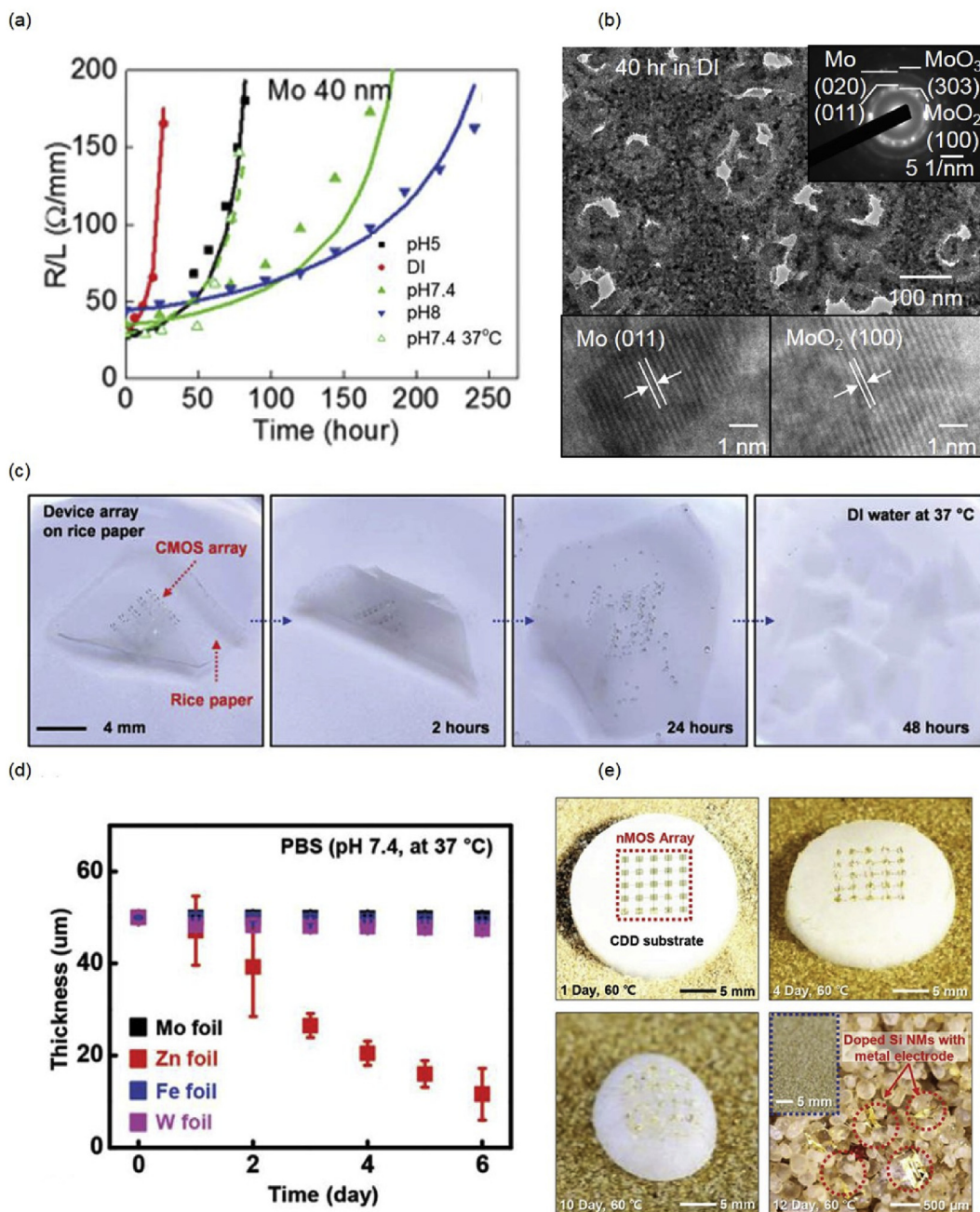

Fig. 2. (a) Dissolution behavior of Mo thin film in DI water and Hanks' solutions with various pH, at both room temperature and 37 °C, with the solid lines representing the modeling dissolution behavior; (b) TEM characterization of Mo thin film after dissolution in DI water for 40 hours; (c) Optical images of dissolution of CMOS array at various stages on the rice paper in DI water at 37 °C; (d) Dissolution kinetics of metal foils in phosphate buffered solutions (pH 7.4, 37 °C); (e) Optical images of sublimation of the CDD substrate and self-destruction of the electronics after 1, 4, 10, and 12 days at 60 °C. Reprinted with permissions from Refs. [28–30, 34].

2.4. Substrate and encapsulation materials

Biodegradable polymers that have been extensively studied are excellent substrate materials, including poly lactic-glycolic acid (PLGA), a copolymer of polylactic acid (PLA) and polyglycolic acid (PGA), polycaprolactone (PCL), silk fibroin, rice paper, poly (1,8-octanediol-co-citrate) (POC), cellulose nanofibril paper, etc. [1,30–32] Electronics built on biodegradable polymeric substrates undergoes device disintegration as well as materials dissolution when comes into contact with aqueous solutions because of the swelling of the polymers. As shown in Fig. 2(c), the rice paper goes through rapid water intake and swelling, thereby disintegrating the electronics [30]. Polymers with slower swelling rates are therefore probably more desirable in order to maintain device performance for a certain lifetime (a few days to weeks) before functional failure. Metallic substrates offer alternative options, as they have the advantages of being dimensionally stable, i.e., they do not swell in biofluids. Metal thin foils of Mo, Fe, W and Zn are investigated as substrates for transient electronics, and the results show that dissolution rates in phosphate buffered solutions are 0.02, 3.5, 0.08, and 0.15 μm.day^{-1} for Mo, Zn, Fe, and W, respectively, as shown in Fig. 2(d) [28].

Stimuli-responsive polymeric materials as substrate materials can offer more versatile transience modes not only in aqueous solution but also in ambient atmosphere, as well as precise control of the degradation initiation. Demonstrated substrate materials with device integration include moisture responsive polyanhydrides [33], temperature responsive materials (cyclododecane (CDD) [34] and methanesulfonic acid/wax [35] composites), and ultraviolet (UV) light responsive materials (photo-acid generator/cyclic poly(phthalaldehyde) (PAG/cPPA)) [36], enabling fully or partially triggered degradation of electronic systems. CDD substrate that sublimes at 60 °C is shown in Fig. 2(e) [34]. Sublimating materials usually have extremely low water solubility and permeability rates which could also possibly be used as encapsulating layers for transient devices in aqueous solutions.

Moreover, biodegradable encapsulation materials represent another critical component which defines the functional lifetime of biodegradable devices. Clinical requirements of device operational timeframes could range from a few days to a couple of weeks. Although biodegradable polymers can serve as encapsulation layers, the high water permeation rates typically cause a fast degradation of the electrically active components, e.g. Mg thin film encapsulated with 5 μm PLGA degrades within 10 min in phosphate buffered solutions at room temperature [23]. Tuning the crystallinity, chemistry, composition and thickness of biopolymers can extend the lifetime, e.g. silk fibroin with high crystallinity can prolong the lifetime of the Mg thin film to ~90 hours [1]; specially synthesized polyanhydride enables a stable operation of intracranial pressure sensor for up to 3 days [18]. Thin film dissolvable oxides are alternative choices. Although the single layer oxide results in a fast dissolution due to the presence of pinholes depending on the deposition conditions, e.g. Mg with 200 nm SiO_2 encapsulation degrades within 1 min in phosphate buffered saline, the combination of alternating SiO_2 and Si_3N_4 layers can extend the lifetime of Mg up to 10 days. Combination of oxide layers and biopolymers is expected to further prolong the functional timeframes, as suggested in the encapsulation studies for organic light emitting diode (OLED) devices [37]. Recent studies have also suggested that the utilization of mono-Si thin film (1.5 μm) as the encapsulation layer can significantly extend the working lifetime of device materials, e.g. Mg thin film remains intact after 60 days in the phosphate buffered solution at 37 °C [23].

2.5. Modeling of dissolution rates

As the dissolution rate is one critical property for biodegradable materials, it is important to have modeling tools that can capture the dissolution behavior and predict the lifetime at both materials and device levels. Considering the complexity of dissolution kinetics and the possible mismatch between the mass change and conductivity change of the materials due to the formation of the non-uniform microstructure (e.g. micro-pores), a simplified one-dimensional reactive diffusion model has been proposed to capture the overall dissolution kinetics of biodegradable materials. The model is able to extract important parameters from measured data that are not existing in the current literature, and can potentially predict the degradation rates of materials under similar conditions, therefore providing critical design guidelines for device integration [1,3,38]. In this model, water concentration w(y, t) at location y and time t follows the reactive diffusion equation, with y = 0 representing the bottom side of the material layer:

$$D\frac{\partial^2 w}{\partial^2 y} - kw = \frac{\partial w}{\partial t} \quad (0 \leq y \leq h_0) \tag{1}$$

where D and k are the diffusivity of water and reaction constant respectively. With boundary conditions assuming a constant water concentration (w_0) at the top surface of the material $w|_{y=h0} = w_0$ ($w_0 = 1\,\text{g cm}^{-3}$) and zero water flux $\partial w/\partial t|_{y=0} = 0$ at the bottom surface, and zero initial water concentration $w|_{t=0} = 0$ ($0 \leq y < h_0$), the analytical solution to Equation (1) can be obtained:

$$h/h_0 \approx 1\text{-}t/t_c \tag{2}$$

where h_0 is the initial thickness and $t_c = h_0 q \rho M_{H2O}(\sqrt{kD}\ w_0 M)^{-1}\tanh^{-1}\sqrt{kh_0^2/D}$ is the critical time when the thickness reaches zero, ρ is the mass density of transient materials, and M and M_{H2O} are the molar masses of transient materials and water, respectively. Dissolution rates can then be defined as $v_{dissolution} = -dh/dt$. As the two free parameters D and k are not available in the literature data, they are acquired by fitting the model to the measured dissolution curves. The calculated rates through reactive diffusion model can be used to predict material dissolution behavior for the same conditions later. Such reactive diffusion model has been applied to capture the dissolution kinetics for single crystal Si, SiO_2, and dissolvable metals (solid lines in Fig. 2(a)). More details can be found in a recent review [3].

Moreover, as the dissolution rates are greatly affected by the ion species and concentrations in the aqueous environments which cannot be easily addressed by the reactive diffusion model, empirical expressions have also been adopted to describe the influence of ions (OH^-, Cl^-, and HPO_4^{2-}) and doping levels on dissolution rates of mono-Si, poly-Si, a-Si, Ge and SiGe [2,14,24,27]. An example of the empirical equation describing the pH-dependent dissolution of mono-Si is shown in Equation (3), where k_0 is the reaction constant, k_B is the Boltzmann constant and E_A is the activation energy. Here, k_0 and E_A are determined by fitting the model with measured data. In a generalization of the empirical model, the exponent index of the reactants (e.g. $[OH]^-$) can also be extracted by fitting. More details can be found in the cited papers [2,15,24].

$$v_{dissolution} = k_0 [H_2O]^4 \left[OH^-\right]^{1/4} e^{-E_A/k_B T} \tag{3}$$

3. Device fabrication techniques

As the constituents of biodegradable electronics, especially the polymeric substrate materials, are sensitive to temperature, solvent or water, novel fabrication schemes instead of conventional photolithography process are therefore required to achieve device integration. Most of the demonstrated biodegradable electronics are based on mono-Si NMs because of its excellent electronic properties. Transfer printing technique has been developed to harvest high-quality mono-Si NMs from a SOI source wafer onto a biodegradable substrate [1,39]. The metallic and dielectric layers have been realized by deposition through a stencil mask in the first demonstration of transient electronics [1]. To improve the fabrication capability, a 2-step transfer printing process is proposed, as shown in Fig. 3(a) [30]. A full device is fabricated on a silicon/poly(methyl methacrylate)/diluted polyimide (Si/PMMA/D-PI) substrate through conventional photolithography as the substrate and device materials can remain stable through the process. The device is covered with an extra D-PI layer on top, and both the top and bottom D-PI layers are patterned into a mesh type to serve as supporting layers for transfer printing. PDMS is then used to pick up the device after etching the sacrificial PMMA layer in acetone, followed by the removal of the bottom D-PI layer through reactive ion etching (RIE). The device is finally achieved on a PLGA substrate after etching the top D-PI layer. The process provides a method to realize lab-scale high-performance transient device.

In order to further achieve integrated biodegradable electronic circuits with more complexity, the foundry-based process offers a possible route. Water-soluble integrated circuit at the 90 nm node with tungsten contacts has been achieved through foundry compatible process using SOI wafers [16]. The circuit has been realized by thinning of the wafer down to 1 μm and transfer-printing onto a silk fibroin substrate [16]. Alternatively, device architectures of silicon complementary metal-oxide-semiconductor (CMOS) arrays can be fabricated on SOI wafers, and released by anisotropic etching in potassium hydroxide (KOH) or tetramethyl-lammonium hydroxide (TMAH) solutions as shown in Fig. 3(b) [17]. SiN_x is used as the anchors and etching barriers to protect the device beneath. The device is then transfer-printed onto a PLGA substrate followed by planarization and metallization techniques to achieve functional systems with excellent electrical characteristics [17].

Besides fabrication of Si CMOS devices, printing of biodegradable metallic components has also been developed for high-speed and low-cost manufacturing of biodegradable antennas and green electronics. Initial attempt of preparing conductive pastes by simply mixing biodegradable metal powders and biodegradable polymers was limited by the relatively low conductivity due to the presence of surface oxides [40]. Ball milling and fast photonic sintering, evaporation-condensation-mediated laser printing, and acid treatment have been proposed to remove surface oxides and achieve highly conductive circuits based on zinc nanoparticles (Zn NPs) [41–43]. Fig. 3(c) shows the schematic printing process for evaporation-condensation-mediated laser printing [42]. Zn NP suspension is first coated on a transparent glass slide, followed by a high-speed continuous-wave (CW) fiber laser irradiation, with Zn coated side gently pressed onto a sodium carboxymethylcellulose (Na-CMC) substrate. The printed Zn conductors show excellent electrical conductivity ($\sim 1.1 \times 10^6 \, S \, m^{-1}$), and strain gauges based on the printing method are successfully demonstrated suggesting potential applications in various eco-friendly circuits.

4. Demonstrated biodegradable devices

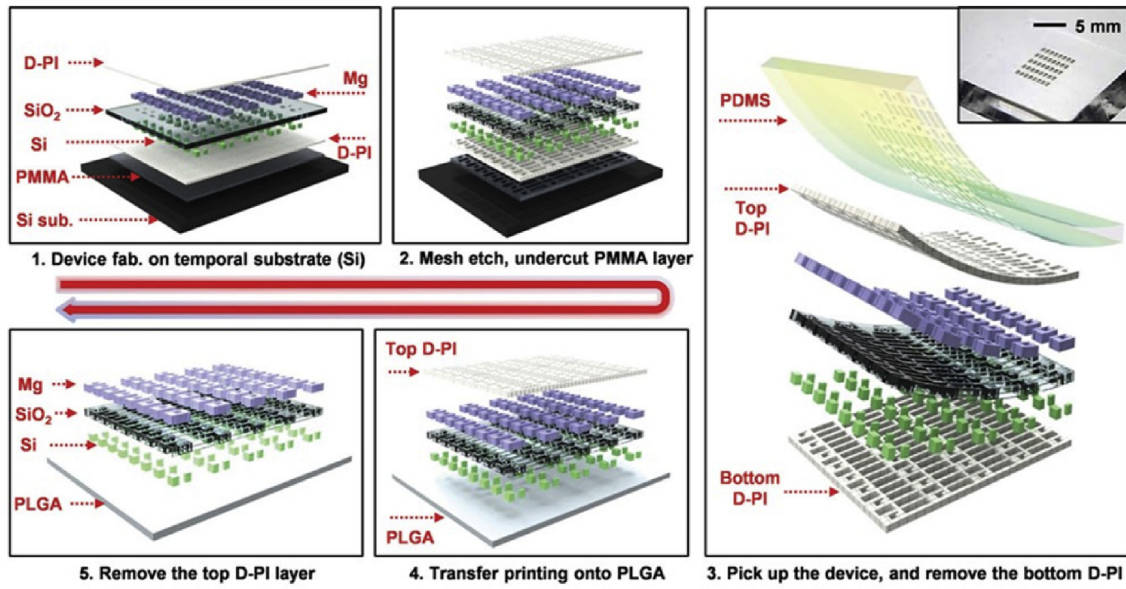The studies of biodegradable materials and novel fabrication

strategies enable integration of various transient functional systems. Demonstrated biodegradable devices are categorized into fully degradable devices and partially degradable devices. Devices capable of complete degradation have the advantages of converting all the constituent materials into resorbable ions or monomers, which eliminates unecessary device loads and is suitable for *in vivo* application without any materials retention. Demonstrated devices include arrays of basic building blocks for integrated circuits (resistors, inductors, capacitors, diodes and transistors) [1], thermal therapy systems to prevent post-surgery infection [1], temperature sensor [1,18,44], dissolvable stretchable electrophysiological and pH sensors [31], implantable drug delivery systems with programmable release [22,45], bioresorbable electronic stent [46], bioresorbable intracranial pressure sensor [18], bioresorbable neural recording system [19], degradable power devices (radio frequency electronics [20], zinc oxides (ZnO) piezoelectric energy harvester [25], super capacitor [47], and battery [21]), etc. On the other hand, partially biodegradable electronics has also been developed targeting edible and eco-friendly applications, including organic thin film transistor on PLGA substrates [11], eco-friendly transistors based on totally disintegrable and biocompatible semiconducting polymers on cellulose substrate [26], high performance green electronics on biodegradable cellulose nanofibril paper [32], edible electronics (circuits [48], supercapacitor [49], and battery [50,51]), etc. Most demonstrated devices are dissolvable or disintegrable in aqueous solutions with rates defined by the dissolution rates of active electronic components or encapsulation layers. Maintaining a stable device performance once deployed in aqueous solutions remains as a critical challenge, as most device components experience fast dissolution and disintegration, and lose performance within a short time, which cannot satisfy clinical requirements of a lifetime that could be up to several weeks. Current strategies addressing the issue include utilizing materials with slow degradation rates (e.g. doped Si, Mo) and encapsulation layers with low water permeability (e.g. hydrophobic biopolymers, Si membrane, alternating layers of dielectric materials), which enables recent developments of silicon electronics capable of chronic *in vivo* monitoring (will be discussed in details later). Moreover, electronics capable of triggered transience based on stimuli-responsive materials has been explored for non-biological applications (e.g. data-secure hardware). Investigated trigger stimuli include moisture [33], temperature [34,35], UV radiation [36], etc. In the following sections, a representative platform will be first introduced demonstrating the concept of the fully biodegradable electronics, followed by recent developments of bioresorbable silicon devices that achieve *in vivo* chronic monitoring of intracranial pressure and electrical activity from the cerebral cortex. The biodegradable power source as an important component for transient electronics will also be discussed.

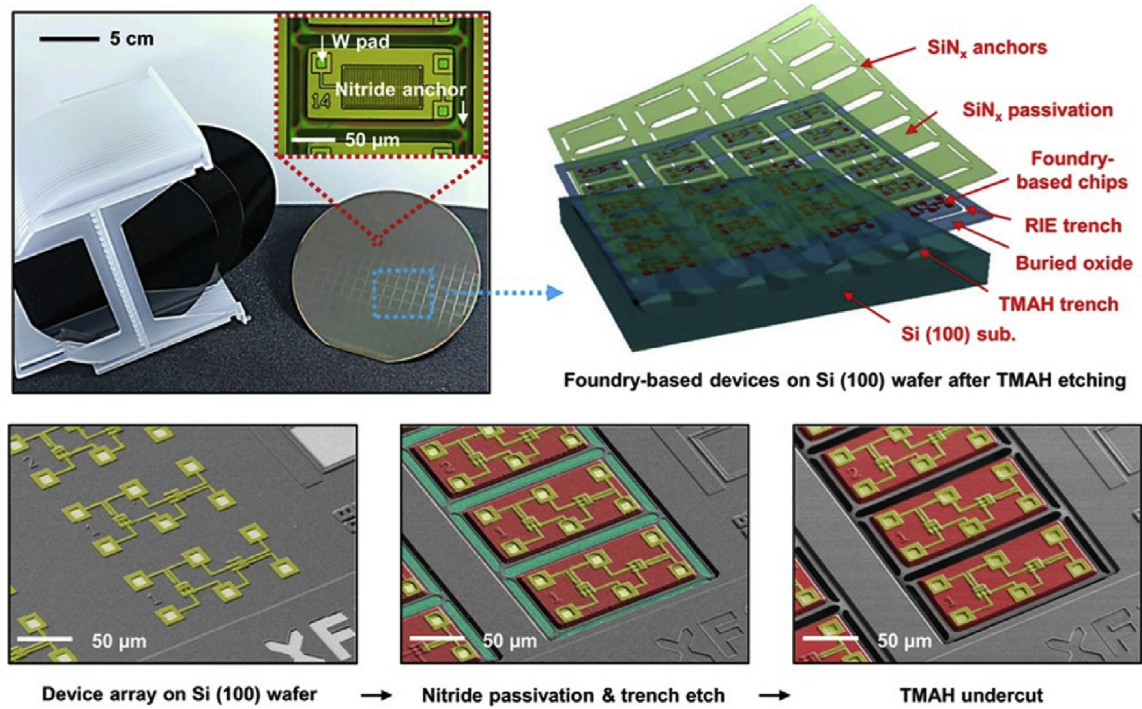### 4.1. Representative biodegradable platform

A representative fully transient device platform demonstrating the concept appears in Fig. 4(a), consisting of transistors, diodes, inductors, capacitors, resistors with interconnects and interlayer dielectrics [1]. The materials involve mono-Si NMs (semiconductor), Mg (conductor), MgO (dielectric layer) and silk fibroin (substrate and encapsulation), as shown in Fig. 4(b). The electrical characteristics of key components built with biodegradable materials appear in Fig. 4 (c) and (d). The performance of the transistors compares favorably to that of counterparts formed with non-degradable materials. The platform disintegrates immediately when immersed in DI water and dissolves after 10 min, as shown in Fig. 4(e). As the fast disintegration compromises the device performance, an encapsulation layer can be introduced to overcome
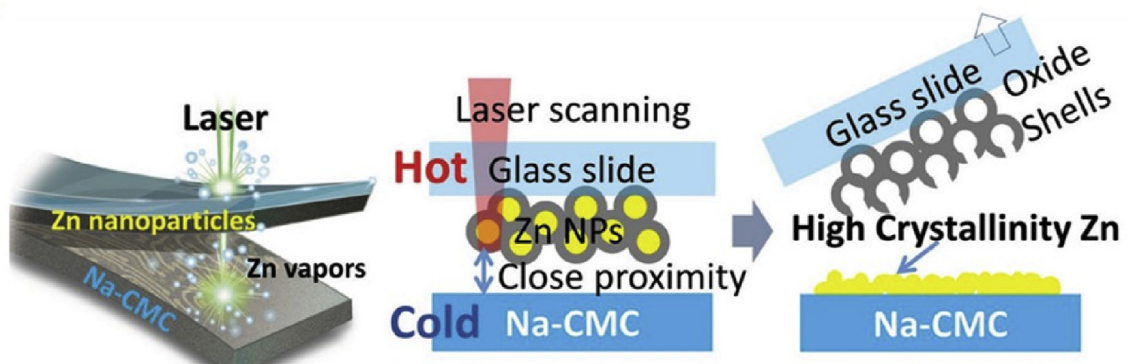
(a)

1. Device fab. on temporal substrate (Si)   2. Mesh etch, undercut PMMA layer

5. Remove the top D-PI layer   4. Transfer printing onto PLGA   3. Pick up the device, and remove the bottom D-PI

(b)

Foundry-based devices on Si (100) wafer after TMAH etching

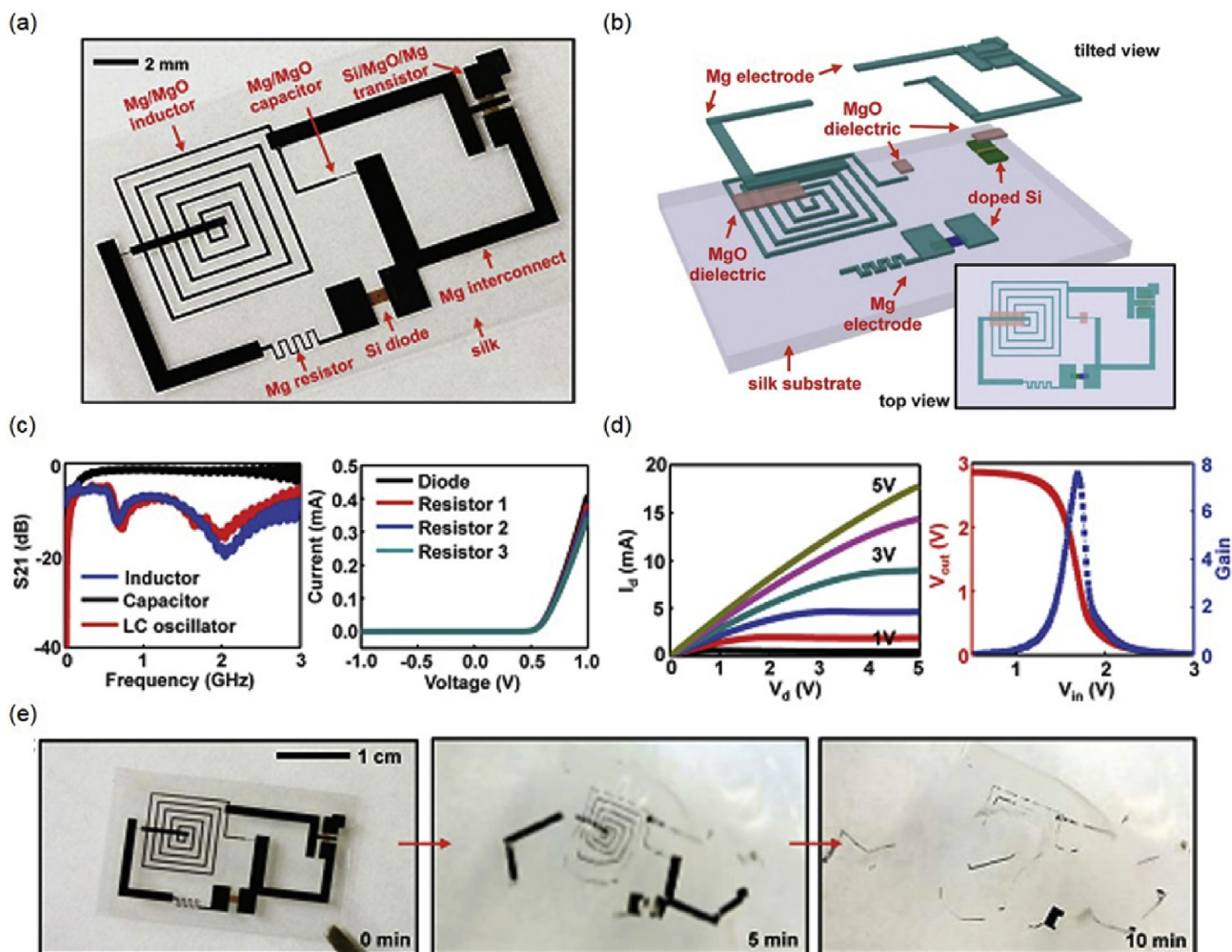Device array on Si (100) wafer   →   Nitride passivation & trench etch   →   TMAH undercut

(c)

Fig. 4. (a) Image of a representative platform for transient electronic device; (b) Exploded illustration of the device; (c) (left) Electrical measurements of an inductor (blue), capacitor (black), and LC oscillator (red), and (right) current-voltage (I-V) characteristics of diodes with Mg electrodes; (d) (left) I-V characteristics of a representative n-channel MOSFET, (right) and the transfer characteristic of an inverter. (e) Images of the dissolution of the platform at different stages in DI Water. Reprinted with permissions from Ref. [1].
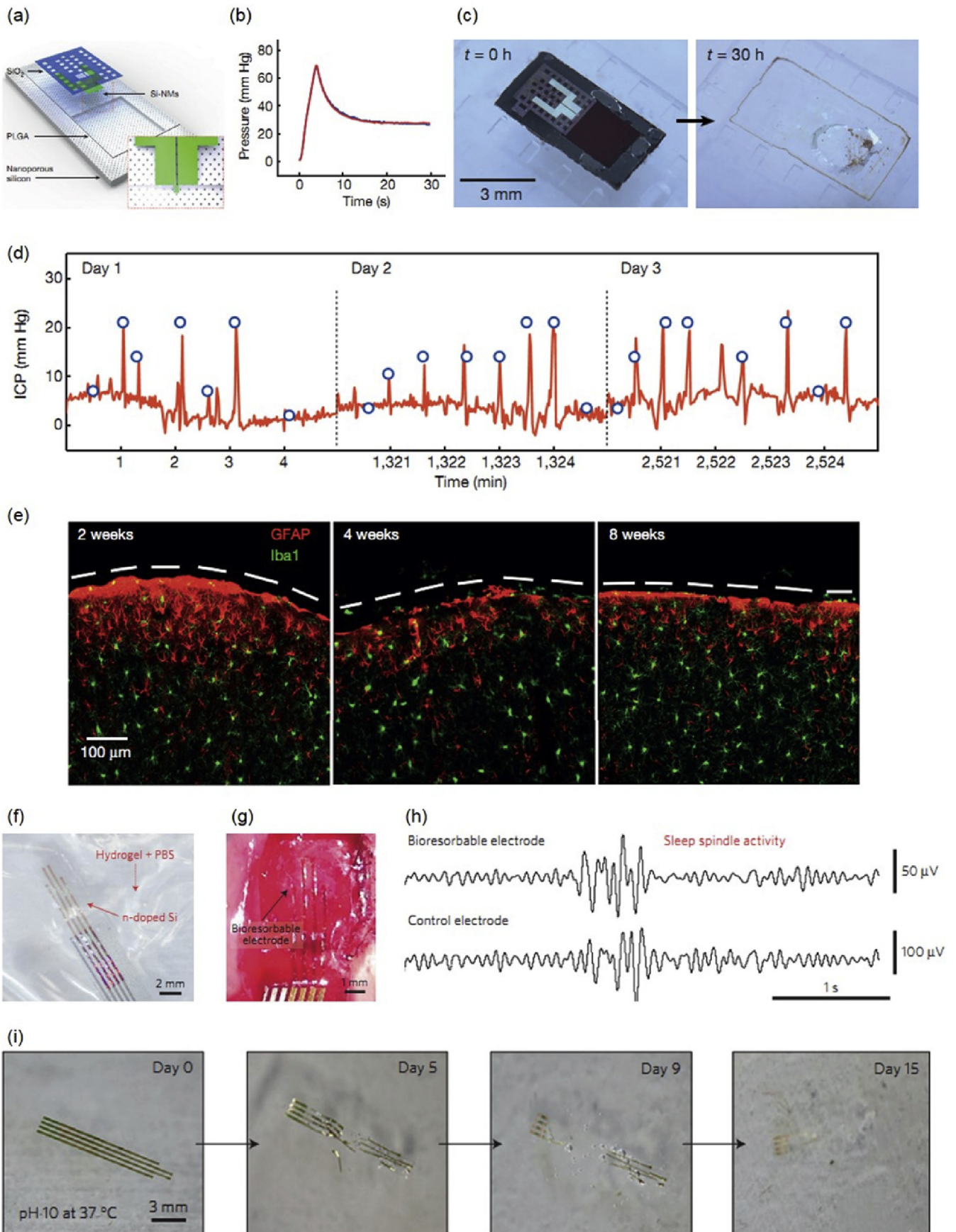
the issue, e.g. degradation rates of silk fibroin can be programed over a wide range of time scale. By applying the encapsulation layer, the n-channel metal oxide semiconductor field-effect transistors (MOSFETs) demonstrate a 2-stage transience, in the sense that the encapsulation layer (silk fibroin and MgO) defines the first time scale of stable operation (~90 h) followed by a fast degradation defined by the Mg electrode, suggesting that the transient behavior can be engineered to be decoupled from the device-level function. The biocompatibility of the materials has been investigated through implantation in the subdermal region on BALB/c mice models, and no significant inflammatory reactions was found after 3 weeks. Transient thermal therapy device consisting of inductive coils (Mg) and resistive micro-heaters (doped Si NMs) on a silk substrate has been used to control surgical site infections, to demonstrate the potential application of transient electronics as biomedical devices [1].

4.2. Bioresorbable silicon electronics

Bioresorbable silicon electronics enables exceptional opportunities to deploy advanced implantable monitoring systems that avoid potential infection risks associated with surgical retrieval procedure. The schematic illustration of a bioresorbable system capable of continuous monitoring of intracranial pressure and temperature essential to the treatment of traumatic brain injury (TBI) is given in Fig. 5(a) [18]. The system involves a PLGA membrane on top of a supporting substrate of nanoporous Si ($60-80 \, \mu m$ thick) which has the advantage of fast degradation. A square of trench ($30-40 \, \mu m$ in depth) is etched onto the surface of the substrate. The deflection of the PLGA membrane associated with the pressure changes in the adjacent biofluids can therefore be captured, due to the presence of the air cavity. A serpentine Si NM as the piezoresistive element is transfer-printed on the edge of the

Fig. 3. (a) 2-step transfer printing procedure of transient electronic circuits: (upper left) defining a mesh type structure allowing the undercut of sacrificial PMMA layer to release the entire device (upper middle), retrieving the released device onto a PDMS stamp (right) followed by the removal of the bottom D-PI layer, transfer printing onto a PLGA substrate (lower middle), and final RIE etching of the top D-PI layer (lower left); (b) Device configuration and release procedures of wafer-scale, ultrathin silicon components for transient electronics. The bottom individual frames correspond to: (left) the unprocessed wafer (device arrays colored with gold), (center) the wafer after passivation and trench etching (the released region of individual device blocks colored with red, and the underlying silicon (100) handle wafer colored with cyan), and (Right) the wafer after TMAH undercut etching; (c) Schematic illustration of evaporation-condensation-mediated laser printing: (left) irradiation of pre-coated Zn NPs ($2.5-5 \, \mu m$) by a high speed scanning laser, (center) glass slide with Zn NPs gently pressed on to the Na-CMC substrate for laser irradiation, (right) Zn conductors with high crystallinity obtained on the Na-CMC substrate. Reprinted with permissions from Refs. [17, 30, 42].

(a)

(b)

(c) t = 0 h   t = 30 h   3 mm

(d)

(e) 2 weeks   4 weeks   8 weeks   GFAP   Iba1   100 µm

(f)   (g)   (h)

(i) Day 0   Day 5   Day 9   Day 15   pH 10 at 37 °C   3 mm

PLGA membrane, and the resistance of the Si NM increases linearly as a function of the pressure in the range relevant to intracranial monitoring (0—70 mm Hg) [18]. An outer passivation layer of SiO_2 provides electrical insulation and corrosion barrier against biofluids. The electronic platform is able to precisely measure the pressure and temperature on a rat model, which compares favorably to those measured by a conventional non-degradable device, as the pressure measurements shown in Fig. 5(b). The device is fully degradable in aqueous solutions, and the accelerated dissolution process in a buffer solution (pH 12) is given in Fig. 5(c). With a specially synthesized polyanhydride encapsulation layer (~120 μm), the pressure sensor enables wireless, stable, and continuous monitoring of intracranial pressure on live and freely moving rats for up to 3 days, and the accuracy and sensitivity of the measurements are comparable to those of a standard non-degradable wired sensor (Fig. 5(d)). Beyond 3 days, water tends to permeate through the encapsulation layer into the electrical connection regions and air cavity, and as a result degrades the performance. With the same polyanhydride encapsulation layer, the measurements from a temperature sensor without the air cavity under similar conditions can offer a stable operation for up to 6 days. The operation timeframes of the devices are relevant for clinical use, as the intracranial pressure and temperature are typically continuously monitored for several days after TBI. As shown in Fig. 5(e), the immunohistochemistry studies of brain tissues after implantation of 2, 4 and 8 weeks suggest that both the device and its degradable by-products have excellent biocompatibility, and no significant immune reaction is observed at the implantation site.

Bioresorbable Si electronics as direct electrical interfaces to the brain capble of neurophysiologic monitoring with multiplexing capabilities has also been proposed for diagnosing and treating neural disorders such as epilepsy [19]. Such device could be important for mapping and monitoring the brain functions before and during neurosurgery, as well as post-surgery monitoring. Localization of neural networks could take several weeks, and recording electrodes in the biodegradable format can eliminate risks and costs associated with the device removal procedure. Here, Si NMs serve as the neural electrode materials as well as the backplane transistors that allow high-speed multiplexing. Highly doped Si NMs are capable of being stable and ultimate bioresorbable due to its relatively slower dissolution rates compared to metals and slightly doped Si. The representative passive neural electrode array appears in Fig. 5(f). Si NMs are transfer-printed onto a PLGA substrate with an outer SiO_2 passivation layer defining the sensing area and serving as a barrier against biofluids. The device arrays are able to perform high-fidelity recording of electrocorticography (ECoG), subdermal encephalograms (EEG) and evoked potentials (Fig. 5(g)). The *in vivo* neural signal test is conducted in an adult rat model applied with anesthetization. As shown in Fig. 5(h), the sleep spindle activity measured by the bioresorbable electrodes compares favorably to that measured by a conventional stainless steel electrode. Passive neural electrodes based on highly-doped Si are able to perform chronic neural interface recording up to 33 days due to the relatively slow and controlled degradation rates. The long lifespan and ultimate transient capability are critically important for long time monitoring,

e.g. localization of epileptic networks takes 1—3 weeks. To minimize the number of wires for external data acquisition, multiplexed neural arrays with Si NMs (recording interface and backplane transistors), Mo (interconnes) and $SiO_2/Si_3N_4/SiO_2$ (encapsulation and interlayer dielectrics) on PLGA are also achieved for high-resolution and high-channel-count neural recording. It is worth noting that the encapsulation layer is critical serving as a barrier against current leakage caused by the permeation of biofluids. The 64-channel multiplexed recording array enables *in vivo* measurements of the propagation of neural waves associated with epileptic spikes and discharges as well as low-amplitude evoked cortical activity, with high signal to noise ratio (SNR). Device system is fully dissolvable in aqueous solutions, as the accelerated dissolution test in a buffer solution (pH 10) of the passive electrodes given in Fig. 5(i). Double-label immunohistochemistry reveals no significant tissue reaction at 4 weeks post-implant compared to that of conventional electrodes with clinical standards.

### 4.3. Biodegradable power sources

The biodegradable power supply is an indispensable component for biodegradable electronic systems to achieve potential electrical functions, including wireless communication, stimulation, sensing, etc. Proposed strategies range from fully degradable radio frequency (RF) power electronics [20], Si based photovoltaics [1], piezoelectric energy harvesters [25], supercapacitors [47], and battery systems [21]. Radio frequency communication is one attractive technology for biomedical application which is capable of both power supply and data transmission. A full wave rectifying circuit based on biodegradable materials has been achieved using Si NM (semiconductor), Mg (metal), SiO_2 (dielectric layer) and silk substrate materials [20]. The electronic system consists of resistors, capacitors, diodes, Mg receiving antenna, and a red LED for function demonstration, as shown in Fig. 6 (a) and (b). The system can wirelessly harvest energy from an external RF transmitter (at a distance ~2 m) and supply enough power to lighten the red LED, as shown in Fig. 6(b). The whole device is again fully degradable in DI water at room temperature, as shown Fig. 6(c).

Alternatively, battery systems offer another power solution as it does not rely on external circuits and the deployment can be more convenient. Current research of bio-battery systems are mostly focused on galvanic cells using metallic electrodes, e.g. Mg and Zn, due to their excellent biocompatibility and high energy density. Reported systems include fully biodegradable Mg-Mo battery systems [21]; and partially degradable batteries: Zn-Cu cells for prolonged *in vivo* monitoring [52], Mg-Fe batteries [53], and Mg-air batteries utilizing silk fibroin or gel electrolyte [54—56]. Biobatteries with non-metallic electrode materials have also been proposed, such as edible sodium ion batteries [50,51], enzymatic fuel cells [57], etc.

As the fully biodegradable battery has the advantage of eliminating potential retention of materials for *in vivo* use, a representative battery system capable of complete degradation is given in Fig. 6(d) [21]. The battery module consists of 4 Mg-Mo cells encased with polyanhydride materials, and is able to provide an output voltage up to 1.6 V for around 6 h at a discharge current density of

---

Fig. 5. (a) Schematic illustration of a bioresorbable intracranial pressure sensor, with the inset showing the location of the Si-NM strain gauge; (b) Pressure as a function of time measured by a commercial pressure sensor (blue) and a calibrated bioresorbable device (red); (c) Images of accelerated dissolution of a bioresorbable pressure sensor in a buffer solution (pH 12) enclosed in a PDMS chamber at room temperature; (d) *In vivo* intracranial pressure measurements for 3 days on a rat model using the device with polyanhydride encapsulation; (e) Confocal fluorescence images of the cortical surface at 2, 4 and 8 weeks (dashed line indicates the site of dissolved device), with glial fibrillary acidic protein (GFAP) to detect astrocytes (red), and ionized calcium-binding adaptor molecule 1 (Iba1) to identify microglia/macrophages (green); (f) Image of the passive bioresorbable neural electrode array; (g) Photograph of a passive four-channel bioresorbable neural device on the cortical surface of a rat; (h) Sleep spindles recorded by bioresorbable passive neural array and the conventional stainless steel electrode as a control on the cortical surface; (i) Accelerated dissolution of a passive bioresorbable neural device at various stages in a buffer solution (pH 10) at 37 °C. Reprinted with permissions from Refs. [18, 19].
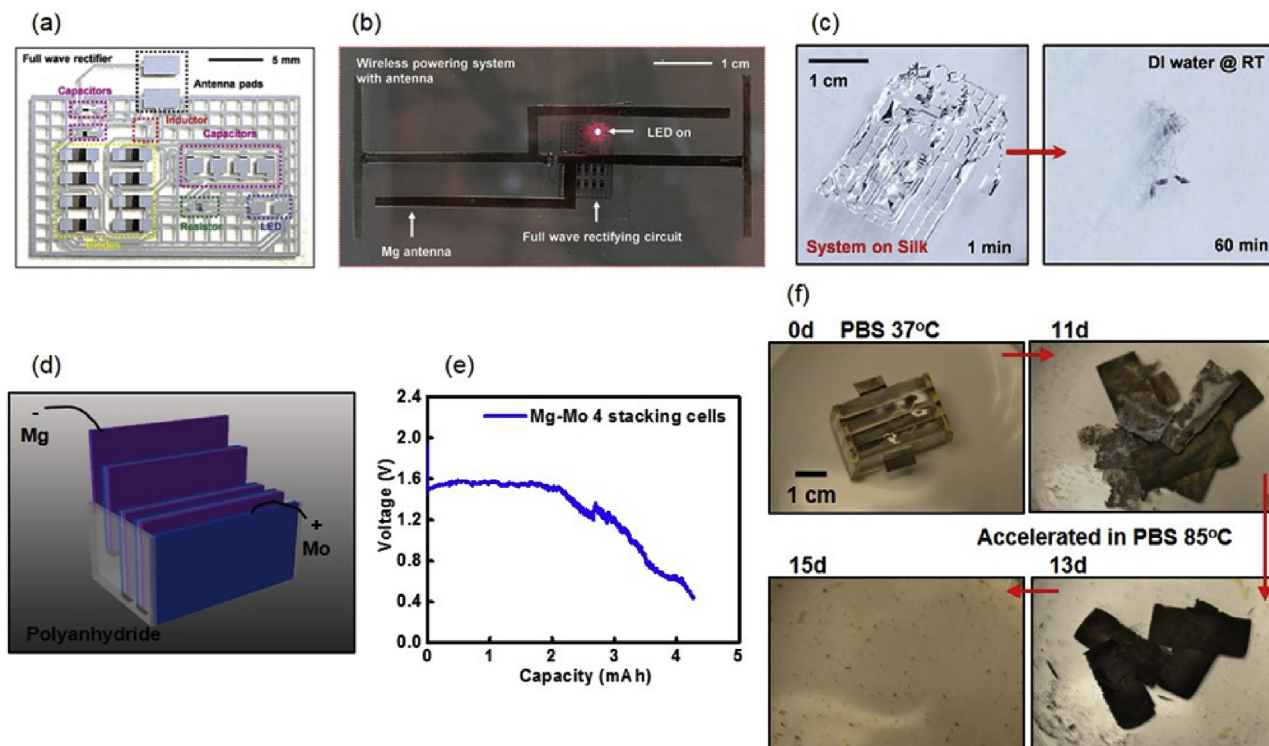
Fig. 6. (a) Photograph of a full wave rectifying circuit built with biodegradable materials, including Si NM, Mg, SiO$_2$ and silk substrate; (b) Image of the full wave rectifying circuit wirelessly powering an LED with a Mg RF receiver; (c) Dissolution of a rectifying circuit in DI water after 1 and 60 min; (d) Schematic illustration of a battery system with 4 Mg-Mo cells in series; (e) Performance of a battery system with 4 Mg-Mo cells (discharge current density 0.1 mA cm^{-2}); (f) Images of the dissolution of a battery system at various stages in phosphate buffered saline. Reprinted with permissions from Refs. [20, 21].

0.1 mA cm^{-2} (Fig. 6(e)). The supplied power is enough to power a LED and a wireless radio circuit indicating practical applications. The battery is fully degradable in phosphate buffered saline as the constituent materials are all water soluble and therefore capble of eliminating uncecessary materials retention, as shown in Fig. 6(f). The on-going research is devoted to further improving the power density, lifetime, and decreasing the size of the battery system.

Besides the aforementioned systems, transient lithium-ion batteries through chemical reactions [58] or chemical/mechanical disintegration [59], primary flow battery with organic quinone redox species [60] have also been explored for eco-friendly applications.

5. Conclusions and perspectives

This review summarizes the up-to-date materials strategies, manufacturing schemes, and device layouts for biodegradable electronics. These studies establish an important baseline for future potential functional systems capable of sensing, stimulating, and monitoring for diagnosing and treating diseases in the brain, cardiac space, spinal systems, etc. Although several essential concepts of biodegradable electronics have been demonstrated both *in vitro* and *in vivo*, the technology is still at the initial phase and many challenges remain. Biodegradable materials database needs to be further expanded including extensive studies of materials chemistry, materials-biology interface, and associated biocompatibility. Stimuli-responsive materials that are compatible with electronic devices are of particular interest, as it can offer versatile modes of transience and achieve precisely control the functional lifetime. Device designs and architectures based on biodegradable materials need to be greatly improved to achieve electrical performance that meets practical clinical standards and at the same time capable of

biodegradation. Novel schemes that enable scalable manufacturing are also critically important to accomplish sophisticated forms of electronic systems. Such emerging technology could potentially provide patients and doctors an important set of tools for fighting human diseases as well as other beneficial values for green electronics, data security, and consumer industries.

References

[1] S.-W. Hwang, H. Tao, D.-H. Kim, H. Cheng, J.-K. Song, E. Rill, M.A. Brenckle, B. Panilaitis, S.M. Won, Y.-S. Kim, Y.M. Song, K.J. Yu, A. Ameen, R. Li, Y. Su, M. Yang, D.L. Kaplan, M.R. Zakin, M.J. Slepian, Y. Huang, F.G. Omenetto, J.A. Rogers, Science 337 (2012) 1640.
[2] S.-W. Hwang, G. Park, H. Cheng, J.-K. Song, S.-K. Kang, L. Yin, J.-H. Kim, F.G. Omenetto, Y. Huang, K.-M. Lee, J.A. Rogers, Adv. Mater. 26 (2014) 1992.
[3] H. Cheng, V. Vepachedu, Theor. Appl. Mech. Lett. 6 (2016) 21.
[4] K.K. Fu, Z. Wang, J. Dai, M. Carter, L. Hu, Chem. Mater. 28 (2016) 3527.
[5] Y. Zhang, B. Lu, H. Xu, X. Feng, Sci. Sin. Phys. Mech. Astron. 46 (044605) (2016).
[6] Z. Wang, K. Fu, Z. Liu, Y. Yao, J. Dai, Y. Wang, B. Liu, L. Hu, Adv. Funct. Mater. 27 (2017) 1605724.
[7] R. Jamshidi, S. Çinar, Y. Chen, N. Hashemi, R. Montazami, J. Polym. Sci. Part B Polym. Phys. 53 (2015) 1603.
[8] P. Tanskanen, Acta Mater. 61 (2013) 1001.
[9] J.A. Lorenzen, Soc. Compass 8 (2014) 1063.
[10] M.D. Luo, A.W. Martinez, S. Chao, H. Florian, A.M. G, J. Microelectromech. S. 23 (2014) 4.
[11] C.J. Bettinger, Z. Bao, Adv. Mater. 22 (2010) 651.
[12] M. Irimia-Vladu, Chem. Soc. Rev. 43 (2014) 588.
[13] Y.H. Jung, T.H. Chang, H. Zhang, C. Yao, Q. Zheng, V.W. Yang, H. Mi, M. Kim, S.J. Cho, D.W. Park, H. Jiang, J. Lee, Y. Qiu, W. Zhou, Z. Cai, S. Gong, Z. Ma, Nat. Commun. 6 (2015) 7170.

[14] S.-W. Hwang, G. Park, C. Edwards, E.A. Corbin, S.-K. Kang, H. Cheng, J.-K. Song, J.-H. Kim, S. Yu, J. Ng, J.E. Lee, J. Kim, C. Yee, B. Bhaduri, Y. Su, F.G. Omennetto, Y. Huang, R. Bashir, L. Goddard, G. Popescu, K.-M. Lee, J.A. Rogers, ACS Nano 8 (2014) 5843.

[15] L. Yin, A.B. Farimani, K. Min, N. Vishal, J. Lam, Y.K. Lee, N.R. Aluru, J.A. Rogers, Adv. Mater. 27 (2015) 1857.

[16] L. Yin, C. Bozler, D.V. Harburg, F. Omenetto, J.A. Rogers, Appl. Phys. Lett. 106 (014105) (2015).

[17] J.-K. Chang, H. Fang, C.A. Bower, E. Song, X. Yu, J.A. Rogers, Proc. Nat. Acad. Sci. 114 (2017) E5522.

[18] S.-K. Kang, R.K.J. Murphy, S.-W. Hwang, S.M. Lee, D.V. Harburg, N.A. Krueger, J. Shin, P. Gamble, H. Cheng, S. Yu, Z. Liu, J.G. McCall, M. Stephen, H. Ying, J. Kim, G. Park, R.C. Webb, C.H. Lee, S. Chung, D.S. Wie, A.D. Gujar, B. Vemulapalli, A.H. Kim, K.-M. Lee, J. Cheng, Y. Huang, S.H. Lee, P.V. Braun, W.Z. Ray, J.A. Rogers, Nature 530 (2016) 71.

[19] K.J. Yu, D. Kuzum, S.-W. Hwang, B.H. Kim, H. Juul, N.H. Kim, S.M. Won, K. Chiang, M. Trumpis, A.G. Richardson, H. Cheng, H. Fang, M. Thompson, H. Bink, D. Talos, K.J. Seo, H.N. Lee, S.-K. Kang, J.-H. Kim, J.Y. Lee, Y. Huang, F.E. Jensen, M.A. Dichter, T.H. Lucas, J. Viventi, B. Litt, J.A. Rogers, Nat. Mater. 15 (2016) 782.

[20] S.-W. Hwang, X. Huang, J.-H. Seo, J.-K. Song, S. Kim, S. Hage-Ali, H.-J. Chung, H. Tao, F.G. Omenetto, Z. Ma, J.A. Rogers, Adv. Mater. 25 (2013) 3526.

[21] L. Yin, X. Huang, H. Xu, Y. Zhang, J. Lam, J. Cheng, J.A. Rogers, Adv. Mater. 26 (2014) 3879.

[22] C.H. Lee, H. Kim, D.V. Harburg, G. Park, Y. Ma, T. Pan, J.S. Kim, N.Y. Lee, B.H. Kim, K.-I. Jang, S.-K. Kang, Y. Huang, J. Kim, K.-M. Lee, C. Leal, J.A. Rogers, NPG Asia Mater. 7 (2015) e227.

[23] Y.K. Lee, K.J. Yu, E. Song, A. Barati Farimani, F. Vitale, Z. Xie, Y. Yoon, Y. Kim, A. Richardson, H. Luan, Y. Wu, X. Xie, T.H. Lucas, K. Crawford, Y. Mei, X. Feng, Y. Huang, B. Litt, N.R. Aluru, L. Yin, J.A. Rogers, ACS Nano (2017), https://doi.org/10.1021/acsnano.7b06697.

[24] S.-K. Kang, G. Park, K. Kim, S.-W. Hwang, H. Cheng, J. Shin, S. Chung, M. Kim, L. Yin, J.C. Lee, K.-M. Lee, J.A. Rogers, ACS Appl. Mater. Interfaces 7 (2015) 9297.

[25] C. Dagdeviren, S.-W. Hwang, Y. Su, S. Kim, H. Cheng, O. Gur, R. Haney, F.G. Omenetto, Y. Huang, J.A. Rogers, Small 9 (2013) 3398.

[26] T. Lei, M. Guan, J. Liu, H.-C. Lin, R. Pfattner, L. Shaw, A.F. McGuire, T.-C. Huang, L. Shao, K.-T. Cheng, J.B.-H. Tok, Z. Bao, Proc. Nat. Acad. Sci. 114 (2017) 5107.

[27] S.-K. Kang, S.-W. Hwang, H. Cheng, S. Yu, B.H. Kim, J.-H. Kim, Y. Huang, J.A. Rogers, Adv. Funct. Mater. 24 (2014) 4427.

[28] S.-K. Kang, S.-W. Hwang, S. Yu, J.-H. Seo, E.A. Corbin, J. Shin, D.S. Wie, R. Bashir, Z. Ma, J.A. Rogers, Adv. Funct. Mater. 25 (2015) 1789.

[29] L. Yin, H. Cheng, S. Mao, R. Haasch, Y. Liu, X. Xie, S.-W. Hwang, H. Jain, S.-K. Kang, Y. Su, R. Li, Y. Huang, J.A. Rogers, Adv. Funct. Mater. 24 (2014) 645.

[30] S.-W. Hwang, J.-K. Song, X. Huang, H. Cheng, S.-K. Kang, B.H. Kim, J.-H. Kim, S. Yu, Y. Huang, J.A. Rogers, Adv. Mater. 26 (2014) 3905.

[31] S.W. Hwang, C.H. Lee, H.Y. Cheng, J.W. Jeong, S.K. Kang, J.H. Kim, J. Shin, J. Yang, Z.J. Liu, G.A. Ameer, Y.G. Huang, J.A. Rogers, Nano Lett. 15 (2015) 2801.

[32] Y. H. Jung, T.-H. Chang, H. Zhang, C. Yao, Q. Zheng, V. W. Yang, H. Mi, M. Kim, S. J. Cho, D.-W. Park, H. Jiang, J. Lee, Y. Qiu, W. Zhou, Z. Cai, S. Gong, Z. Ma, 6, 7170, (2015).

[33] Y. Gao, Y. Zhang, X. Wang, K. Sim, J. Liu, J. Chen, X. Feng, H. Xu, C. Yu, Sci. Adv. 3 (2017).

[34] B.H. Kim, J.-H. Kim, L. Persano, S.-W. Hwang, S. Lee, J. Lee, Y. Yu, Y. Kang, S.M. Won, J. Koo, Y.K. Cho, G. Hur, A. Banks, J.-K. Song, P. Won, Y.M. Song, K.-I. Jang, D. Kang, C.H. Lee, D. Pisignano, J.A. Rogers, Adv. Funct. Mater. 27 (2017)

[35] 1606008.
C.W. Park, S.-K. Kang, H.L. Hernandez, J.A. Kaitz, D.S. Wie, J. Shin, O.P. Lee, N.R. Sottos, J.S. Moore, J.A. Rogers, S.R. White, Adv. Mater. 27 (2015) 3783.

[36] H.L. Hernandez, S.-K. Kang, O.P. Lee, S.-W. Hwang, J.A. Kaitz, B. Inci, C.W. Park, S. Chung, N.R. Sottos, J.S. Moore, J.A. Rogers, S.R. White, Adv. Mater. 26 (2014) 7637.

[37] S. Park, W.M. Yun, L.H. Kim, S. Park, S.H. Kim, C.E. Park, Org. Electron. 14 (2013) 3385.

[38] R. Li, H. Cheng, Y. Su, S.-W. Hwang, L. Yin, H. Tao, M.A. Brenckle, D.-H. Kim, F.G. Omenetto, J.A. Rogers, Y. Huang, Adv. Funct. Mater. 23 (2013) 3106.

[39] M.A. Meitl, Z.-T. Zhu, V. Kumar, K.J. Lee, X. Feng, Y.Y. Huang, I. Adesida, R.G. Nuzzo, J.A. Rogers, Nat. Mater. 5 (2006) 33.

[40] X. Huang, Y. Liu, S.-W. Hwang, S.-K. Kang, D. Patnaik, J.F. Cortes, J.A. Rogers, Adv. Mater. 26 (2014) 7371.

[41] B.K. Mahajan, X. Yu, W. Shou, H. Pan, X. Huang, Small 13 (2017) 1700065.

[42] W. Shou, B.K. Mahajan, B. Ludwig, X. Yu, J. Staggs, X. Huang, H. Pan, Adv. Mater. 29 (2017) 1700172.

[43] Y.K. Lee, J. Kim, Y. Kim, J.W. Kwak, Y. Yoon, J.A. Rogers, Adv. Mater. 29 (2017) 1702665.

[44] G.A. Salvatore, J. Sülzle, F. Dalla Valle, G. Cantarella, F. Robotti, P. Jokic, S. Knobelspies, A. Daus, L. Büthe, L. Petti, N. Kirchgessner, R. Hopf, M. Magno, G. Tröster, Adv. Funct. Mater. 27 (2017) 1702390.

[45] H. Tao, S.-W. Hwang, B. Marelli, B. An, J.E. Moreau, M. Yang, M.A. Brenckle, S. Kim, D.L. Kaplan, J.A. Rogers, F.G. Omenetto, Proc. Nat. Acad. Sci. 111 (2014) 17385.

[46] D. Son, J. Lee, D.J. Lee, R. Ghaffari, S. Yun, S.J. Kim, J.E. Lee, H.R. Cho, S. Yoon, S. Yang, S. Lee, S. Qiao, D. Ling, S. Shin, J.-K. Song, J. Kim, T. Kim, H. Lee, J. Kim, M. Soh, N. Lee, C.S. Hwang, S. Nam, N. Lu, T. Hyeon, S.H. Choi, D.-H. Kim, ACS Nano 9 (2015) 5937.

[47] G. Lee, S.-K. Kang, S.M. Won, P. Gutruf, Y.R. Jeong, J. Koo, S.-S. Lee, J.A. Rogers, J.S. Ha, Adv. Energy Mater. 7 (2017) 1700157.

[48] W. Xu, H. Yang, W. Zeng, T. Houghton, X. Wang, R. Murthy, H. Kim, Y. Lin, M. Mignolet, H. Duan, H. Yu, M. Slepian, H. Jiang, Adv. Mater. Technol. 2 (2017) 1700181.

[49] X. Wang, W. Xu, P. Chatterjee, C. Lv, J. Popovich, Z. Song, L. Dai, M.Y.S. Kalani, S.E. Haydel, H. Jiang, Adv. Mater. Technol. 1 (2016) 1600059.

[50] Y.J. Kim, W. Wu, S.-E. Chun, J.F. Whitacre, C.J. Bettinger, Proc. Nat. Acad. Sci. 110 (52) (2013).

[51] Y.J. Kim, S.-E. Chun, J. Whitacre, C.J. Bettinger, J. Mater. Chem. B 1 (2013) 3781.

[52] P. Nadeau, D. El-Damak, D. Glettig, Y.L. Kong, S. Mo, C. Cleveland, L. Booth, N. Roxhed, R. Langer, A.P. Chandrakasan, G. Traverso, Nat. Biomed. Eng. 1 (0022) (2017).

[53] M. Tsang, A. Armutlulu, A.W. Martinez, S.A.B. Allen, M.G. Allen, Microsys. Nanoeng. 1 (2015) 15024.

[54] X. Jia, Y. Yang, C. Wang, C. Zhao, R. Vijayaraghavan, D.R. MacFarlane, M. Forsyth, G.G. Wallace, ACS Appl. Mater. Interfaces 6 (2014) 21110.

[55] X. Jia, C. Wang, C. Zhao, Y. Ge, G.G. Wallace, Adv. Funct. Mater. 26 (2016) 1454.

[56] X. Jia, C. Wang, V. Ranganathan, B. Napier, C. Yu, Y. Chao, M. Forsyth, F.G. Omenetto, D.R. MacFarlane, G.G. Wallace, ACS Energy Lett. 2 (2017) 831.

[57] Z. Zhu, T. Kin Tam, F. Sun, C. You, Y. H. Percival Zhang, 5, 3026, (2014).

[58] K. Fu, Z. Liu, Y. Yao, Z. Wang, B. Zhao, W. Luo, J. Dai, S.D. Lacey, L. Zhou, F. Shen, M. Kim, L. Swafford, L. Sengupta, L. Hu, Nano Lett. 15 (2015) 4664.

[59] Y. Chen, R. Jamshidi, K. White, S. Çınar, E. Gallegos, N. Hashemi, R. Montazami, J. Polym, Sci. Part B Polym. Phys. 54 (2016) 2021.

[60] J.P. Esquivel, P. Alday, O.A. Ibrahim, B. Fernández, E. Kjeang, N. Sabaté, Adv. Energy Mater. 7 (2017) 1700275.